*M&C 2017 - International Conference on Mathematics & Computational Methods Applied to Nuclear Science & Engineering, Jeju, Korea, April 16-20, 2017, on USB (2017)*

# Fixed-Source and Ex-Core Detector Calculations with SIMULATE5

Tamer Bahadir[a], Matthew M. Giffen[b], Christopher Wells[b]

*(a) Studsvik Scandpower, Inc.: 309 Waverley Oaks Rd, Suite 406, Waltham, MA 02452, USA, tamer.bahadir@studsvik.com*
*(b) Dominion Generation: 5000 Dominion Blvd, Glen Allen, VA, 23060, USA, matthew.m.giffen@dom.com*
*christopher.j.wells@dom.com*

**Abstract** - *During the time that a reactor is brought up to its "critical" condition, the flux distribution in the core is substantially different than that of the critical core and determined, in large part, by the distribution of internal and external neutron sources in the core. One important safety consideration during a reactor start-up is to assure that the distributions of sources and source range detectors are sufficient to monitor the approach to critical. The rate of change of the core flux is often used as a means of determining the incremental reactivity to be inserted as the critical condition is approached. In some cases, ex-core detector response is either directly or indirectly credited with providing operators effective indication that an inadvertent boron dilution is in progress. This paper describes the fixed-source computational capabilities implemented into the Studsvik CMS5 code package to model such events for Pressurized Water Reactors. The intrinsic, natural, neutron sources of irradiated fuel assemblies are computed from the 2D lattice code CASMO5. The 3D, steady-state nodal code, SIMULATE5 solves the fixed-neutron source equations, with the given intrinsic and external, secondary, source distributions using the analytical nodal model. The ex-core detector models implemented in SIMULATE5 are used to compute the detector response and to infer inverse count rate ratio (ICRR). The coupled fixed-source calculations and the ex-core detector models are used for simulating approach to critical events for operating reactors and validated against Monte Carlo calculations as well as plant measurements. It has been shown that CMS5 is an effective tool to predicting the ex-core detector signal during start-ups with and without the external neutron sources in the core. Additionally, it has been demonstrated that the ex-core detector response sensitivity can be improved significantly by properly placed secondary neutron sources in the core.*

## I. INTRODUCTION

During the time that a reactor is brought up to its "critical" condition, the flux distribution in the core is determined, in large part, by the distribution of neutron sources in the core. In a clean core, a start-up source is always used to initiate the chain reaction. In cores containing depleted fuel, there exist many natural sources of neutrons which can be used to initiate the chain reaction. One important safety consideration during a reactor start-up is to assure that the distributions of sources and ex-core and in-core source range detectors are sufficient to monitor the approach to critical. The rate of change of the core flux is often used as a means of determining the incremental reactivity to be inserted as the critical condition is approached. In some cases, ex-core detector response is either directly or indirectly credited with providing operators effective indication that an inadvertent boron dilution is in progress[1].

Pressurized Water Reactor (PWR) ex-core detectors are located outside of the reactor vessel and their signal is mostly driven by the neutrons originating in the peripheral fuel assemblies. Today's low-leakage core designs, with high burned fuel assemblies on the core periphery, and the elimination of the primary and secondary neutron sources severely limits the sensitivity of the ex-core detector signal, especially during approach to criticality events starting from the all-rods-in condition[2,3]. Since the detector response may not be a good indicator of inadvertent approach to criticality, it is important to have tools for analyzing such events and take preventive measures, such as bringing secondary sources back into the core, if necessary.

Most core neutronics calculations use an eigenvalue search (e.g., k-eff) or a coupled neutronic/ thermal-hydraulic search (e.g., power or flow) to determine the steady-state critical condition of a reactor. These calculations are appropriate whenever the flux level is significantly higher than the one generated by start-up sources and naturally-occurring neutron sources. The flux distribution in a sub-critical core is substantially different from that of a critical core, and it is important to treat the neutron source distributions in the calculation of core flux distributions.

This paper describes the fixed-source computational capabilities implemented into the Studsvik CMS5 code package with CASMO5[4] and SIMULATE5[5]. The code package can be used:

1. To study internal and external neutron sources and the placement of external neutron sources within a reactor core,
2. To study ex-core detector responses to movements of control rods and boron dilution events for PWRs and in-

core detector responses to the movements of control rods for Boiling Water Reactors (BWRs).

3. To determine the sub-criticality of the core.

The SIMULATE5 nodal model used with solving the fixed neutron source equations along with the ex-core detector models are described in Section II. The Monte Carlo model, used for validation as well as for computing the ex-core detector weight functions, are also described in Section II. The validation of the fixed-source calculations combined with the ex-core detector model versus the Monte Carlo calculations and the measurement during approach to critical events of operating reactors are presented in Section III. Final conclusions are drawn at the end of the paper in Section IV.

## II. FIXED-SOURCE AND DETECTOR MODELS

### 1. SIMULATE5 Fixed-Source Model

SIMULATE5 is a 3D nodal code that solves the steady-state, multi-group forward diffusion equation, G groups, for a system of parallelepipeds, called nodes. Each node has a square base of fixed size *hx·hx* and an axial height, *hz*, that may vary along the vertical channel.

The multi-group forward diffusion equation for group g (g=1,...,G) is given by

$$D_g \nabla^2 \phi_g - \left(\Sigma_{ag} + \Sigma_{rg}\right)\phi_g + \sum_{\substack{h=1 \\ h \neq g}}^{G} \Sigma_{sgh}\phi_h + \frac{1}{k_{eff}} \sum_{h=1}^{G} \chi_g \nu\Sigma_{fh}\phi_h + S_g^{fix} = 0 \tag{1}$$

where

- $D_g$ - diffusion coefficient,
- $\Sigma_{ag}$ - absorption cross section,
- $\Sigma_{sgh}$ - scattering cross section,
- $\Sigma_{rg}$ - removal cross section,
- $\nu\Sigma_{fg}$ - fission cross section times number of neutrons per fission,
- $\chi_g$ - fission spectrum,
- $k_{eff}$ - effective multiplication constant,
- $S_g^{fix}$ - fixed neutron source.

The cross sections may vary smoothly inside a node in the x and y directions, but not in the z direction. The diffusion coefficient and the fixed neutron source are node-wise uniform.

In a criticality calculation, $k_{eff}$ is the unique largest positive eigenvalue of the problem, and $S_g$ is zero. Since the source-free diffusion equation is homogeneous, there are infinite number of solutions to this equation. The flux level cannot be determined from the diffusion equations itself, and it must be determined from power or flow searches for critical thermal-hydraulic conditions, or the power level must be set from external constraints.

If one wishes to solve the neutron diffusion equation with a known distribution of sources, $S_g$, the equation is no longer homogeneous in the fluxes. This implies that there is one and only one unique distribution of fluxes corresponding to a fixed distribution of sources and a known set of cross sections. It is important to note that the value of $k_{eff}$ in Eq. 1 must be known in order to solve for the flux distributions.

### 2. Fixed-Neutron Sources

The fixed-source term in Eq. 1 can be expanded as

$$S_g^{fix} = \chi_g^{\text{int}} S^{\text{int}} + \chi_g^{ext} S^{ext} \tag{2}$$

where

- $\chi_g^{\text{int}}$ -internal neutron source spectrum,
- $S^{int}$ -internal neutron source,
- $\chi_g^{ext}$ - external neutron source spectrum,
- $S^{ext}$ - external neutron source.

1. Internal neutron sources are due to spontaneous fission and alpha-n reactions, and, hence, are strongly burnup dependent. The internal neutron source is computed by CASMO5 and functionalized in the cross-section library vs. burnup and history parameters in the same manner as cross sections and discontinuity factors. Optionally, the microscopic depletion model of SIMULATE5, which tracks 16 actinides, can be used to compute the internal neutron source term, on the fly, as shown in Eq. 3:

$$S^{\text{int}} = \sum_i \frac{N_i A_i}{NA} (\nu_{\alpha n,i} + \nu_{SF,i}) \tag{3}$$

where

- $N_i$ - the number density of *nuclide-i*,
- $A_i$ - the atomic weight of *nuclide-i*,
- $NA$ - Avogadro's number,
- $\nu_{\alpha n,i}$ - the average neutron yield due to (alpha,n) reactions per gram of *nuclide-i*,
- $\nu_{SF,i,i}$ - the average neutron yield due to spontaneous fission reactions per gram of *nuclide-i*.

The summation over *i* includes all important Pu, Am and Cm isotopes that contribute to the internal neutron sources.

2. External, or secondary, sources, if any in the core, their strength and location are provided by the user.

### 3. Solution of Fixed Neutron Source Problem

In compact matrix form, Eq. 1 can be written as

$$\underline{\underline{D}} \nabla^2 \underline{\phi} + \underline{\underline{\Sigma}}(r) \cdot \underline{\phi}(r) + \underline{S}^{fix} = 0 \tag{4}$$

Integrating Eq. 4 for node *n* yields a neutron balance equation which will be used in the global coupling of the nodes:

$$\sum_{m=1}^{6} \frac{1}{h_{hm}} \underline{J}_{nm} - \underline{\underline{\tilde{\Sigma}}}_n \underline{\bar{\phi}}_n = \underline{S}^{fix} \tag{5}$$

Eq. 5 contains two unknown variables, $J_{nm}$, the net average leakage from node *n* to node *m*, and $\phi_n$, the average flux. To obtain the relation between these two, SIMULATE5 solves the three-dimensional multi-group diffusion equation by the Analytic Nodal Method[5]. The 3D diffusion equations are integrated over the transverse directions to give a coupled set of 1D equations. The transverse leakage is approximated by a quadratic fit of the known average out-leakages of three adjoining nodes. The one-dimensional multi-group equation is converted into G 'one-group' equations by a transformation, employing the eigenvectors of the buckling matrix B[2]. The one-group equation is readily solved, leading to an expression relating the side flux gradient to the side average flux, the node average flux, and the spatial expansion coefficients of the transverse leakage.

By requiring current and flux continuity (or known discontinuity) between two nodes, the net-current as a function of the average fluxes in nodes *n* and *m* becomes:

$$\underline{J}_{nm} = h_{nm} \left( \underline{\underline{C}}_{nm}^{own} \underline{\bar{\phi}}_n + \underline{g}_{nm}^{own} - \underline{\underline{C}}_{nm}^{nei} \underline{\bar{\phi}}_m - \underline{g}_{nm}^{nei} \right) \tag{6}$$

Where C and g are the coupling coefficients. Combining Eq. 6 with the node balance Eq. 5 gives

$$\left[ \sum_{m=1}^{6} \underline{\underline{C}}_{nm}^{own} \right] \underline{\bar{\phi}}_n - \sum_{m=1}^{6} \underline{\underline{C}}_{nm}^{nei} \underline{\bar{\phi}}_m - \underline{\underline{\tilde{\Sigma}}}_n \underline{\bar{\phi}}_n = \underline{S}^{fix} - \sum_{m=1}^{6} \left[ \underline{g}_{nm}^{own} - \underline{g}_{nm}^{nei} \right] \tag{7}$$

where the summation extends over the six adjacent nodes of node n.

The fixed source equation, Eq. 7, may be rewritten in the following form

$$\underline{\bar{\phi}}_n = \sum_{m=1}^{6} \underline{\underline{A}}_{nm} \underline{\bar{\phi}}_m - \underline{b}_n \tag{8}$$

where

$$\left.\begin{aligned} \underline{\underline{\alpha}}_n &= \sum_{m=1}^{6} \underline{\underline{C}}_{nm}^{own} - \underline{\underline{\Sigma}}_n \\ \underline{\underline{A}}_{nm} &= \underline{\underline{\alpha}}_n^{-1} \cdot \underline{\underline{C}}_{nm}^{nei} \\ \underline{b}_n &= \underline{\underline{\alpha}}_n^{-1} \cdot \left( \underline{S}^{fix} - \sum_{m=1}^{6} \left[ \underline{g}_{nm}^{own} - \underline{g}_{nm}^{nei} \right] \right) \end{aligned}\right\} \tag{9}$$

Given a known fixed source, Eq. 9 is solved by the CCSI (Cyclic Chebyshev Semi Iteration) method.

The fixed-source problem is well-defined only if the corresponding homogeneous problem is sub-critical. Consequently, if one attempts to solve the fixed source problem with $k_{eff}$ exactly equal to (or less than) the critical eigenvalue for the given core conditions, the resulting iteration will produce infinitely large fluxes. This is simply a confirmation that without thermal-hydraulic feedback, a critical reactor containing a source will always increase its flux level (i.e., there is no steady state solution.)

For fixed-source cases of real interest, the reactor core will always be subcritical, and there will be only one flux solution. It is important that the user specify that $k_{eff}$ be the best estimate of the critical eigenvalue at the given conditions (e.g., the expected cold clean critical eigenvalue based on past cycle/critical evaluations). The user input $k_{eff}$ accounts for any known bias between the calculated critical eigenvalues and the actual measured critical benchmarks, when such benchmark data is available. Note that a non-zero bias typically exists and is caused by imperfections in the cross sections, and/or cycle specific models, and/or methods.

## 4. PWR Ex-Core Detector Model

The multi-group fluxes obtained from the solution of the fixed-source problem are used for driving the ex-core detector signals for PWRs. Fig.1 shows a simplistic representation of an ex-core detector and its location relative to core components and reactor vessel.

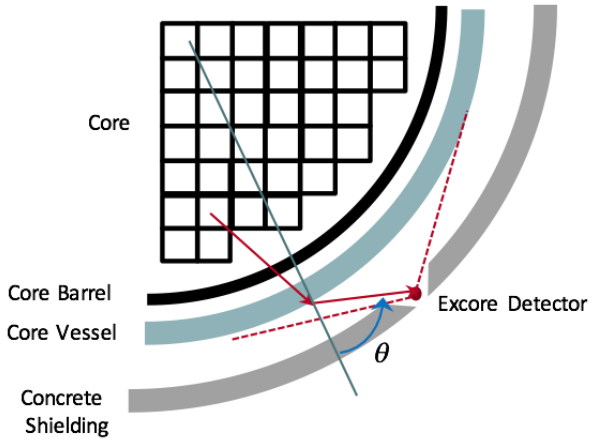


Fig.1 Ex-core detector geometry.

There are two different ex-core detector models available in SIMULATE5:

1. Source Weighted Model[6]: The detector response is computed as a weighted average of the total nodal source:

$$R_d^{3D} = CALIB_d \sum_k a_{d,k} \sum_{ij} r_{d,ij} RPF_{ij,k} \quad (10)$$

where

$R_d$ - detector response of *detector-d*,
$CALIB_d$ - calibration constant *detector-d*,
$a_{d,k}$ - node axial weighting factor,
$r_{d,ij}$ - node radial weighting factor,
$RPF_{ij,k}$ - total, fission and secondary, neutron source in node-*ij*,*k*.

SIMULATE5 can compute the radial weighting factors based on the geometry, using a "double kernel[7]" method to approximate the radial neutron transport from each assembly through core baffle, the vessel, and finally to the detector locations. Alternatively, the radial weighting factors obtained from other sources, such as external transport calculations, can be provided. The axial weighting factors must also be defined by axial zone for each detector.

2. Geometrical Model[8]: The number of epithermal neutrons reaching the ex-core detectors is arrived at by a two-step procedure:
   - Extrapolate the reflector flux, which is already available from the solution of the fixed neutron-source equations for each explicit reflector node, *ij-k*, to the core pressure vessel *segment-s*, with the assumption that there is water between the core baffle and the vessel:

$$\phi_{vessel,k,s} = \phi_{reflector,k,ij} . e^{-\kappa . \Delta r}$$
$$\kappa^2 = \frac{\Sigma_{a1} + \Sigma_r}{D_1} \quad (11)$$

   - Compute how many neutrons will find their way from the surface of the vessel to the detectors for the given core and ex-core geometry:

$$R_d^{3D} = CALIB_d \sum_s \sum_k \phi_{vessel,s,k} \frac{C_\theta}{r_{sd}^2} \quad (12)$$

where

$C_\theta$ - the geometrical term accounting the angular distribution of neutrons exiting the vessel surface and reaching the *detector-d* with the polar angle $\theta$, the angle between the barrel normal and the neutron trajectory to the detector as shown in Fig 1.
$r_{sd}$ - the distance between the ex-core *detector-d* and the vessel *segment-s*.

## 5. BWR Source Range In-Core Detector Model

Although the primary scope of this paper is to describe the use of the fixed-source calculation capability with PWRs, the extension of the model for BWRs is summarized here for completeness.

The main difference in BWR core monitoring during shutdown/start-up is the use of fixed in-core neutron detectors. The SIMULATE5 in-core detector model assumes that the detector is represented by a trace amount of $^{235}U$ and that the microscopic cross-sections and the detector peaking factors are generated in CASMO5 and placed into the neutronics data library. All the mechanics normally used for modeling of LPRMs (Local Power Range Monitors) can be used to model SRMs (Source Range/Start-up Range) or other special purpose detectors.

The response of the detector, which is located in the narrow-narrow corners of four fuel assemblies, is computed as[9]:

$$R_d^{3D} = \frac{1}{4} \sum_{n=1}^{4} \sum_{g=1}^{G} \left( \sigma_{g,n}^{Det,C5} \cdot \frac{\phi_{g,n}^{Det,C5}}{\bar{\phi}_{g,n}^{C5}} \right) \cdot \phi_{g,n}^{Det,S5} \quad (13)$$

where

$\sigma_{g,n}^{Det,C5}$ - Detector microscopic cross-section,
$\phi_{g,n}^{Det,C5} / \bar{\phi}_{g,n}^{C5}$ - CASMO5 detector peaking factor,
$\phi_{g,n}^{Det,S5}$ - SIMULATE5 detector flux.

The multi-group detector constants are found by table interpolation of the library using local conditions (e.g., burnup, void/control rod history, instantaneous void etc.) of an assembly. The corner point flux at the detector location is constructed from the solution of the fixed neutron source equations (Eq. 4) and used as SIMULATE detector fluxes in Eq. 13 above. When a detector spans multiple axial nodes, the flux used in the calculation is computed by performing an axial integration of the detailed, cm-by-cm, axial flux shape available from SIMULATE5[5].

## 6. MCNP5 Benchmark Model

A 3D core model for one of the latest cycles of an operating 3-loop Westinghouse PWR was setup with the Monte Carlo code MCNP5[10].

The MCNP5 models used a heterogeneous core geometry, including fuel, clad, moderator, IFBA coatings, discrete burnable absorbers, control rods, primary neutron sources, and secondary neutron sources. Irradiated fuel compositions and intrinsic neutron sources were specified on a fuel-assembly basis with 16 axial intervals. IFBA patterns and discrete burnable absorber rodlet locations were explicitly modeled. Irradiated burnable absorber material compositions were also modeled using 16 axial intervals.

The ex-core model included top and bottom reflectors, baffle plates, former plates, core barrel, thermal shield, and

reactor vessel. All components were modeled with as-designed dimensions and compositions. Fig. 2 shows the radial and axial cuts of the 3D heterogeneous geometry modeled with MCNP5.

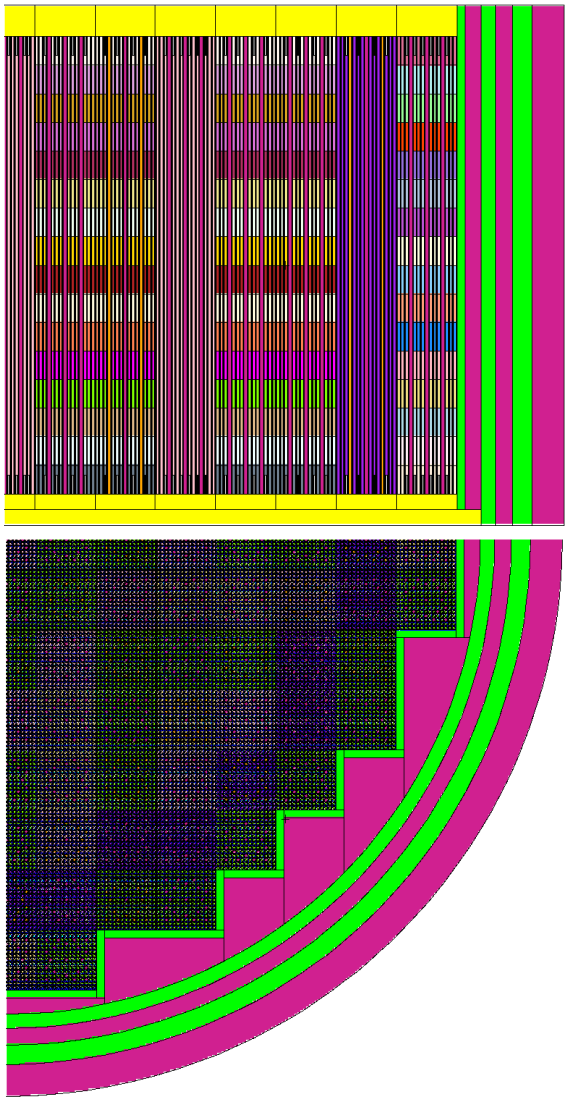

Fig. 2. 3D full core geometry of a 3-loop Westinghouse PWR modeled with MCNP.

The ex-vessel model included the source range detectors and the neutron shield tank. The internal structures of the neutron shield tank were explicitly modeled, including the dry wells that contain the source range detectors.

Irradiated fuel compositions were extracted from CMS5 and included over 200 isotopes. Irradiated fuel neutron source intensities were also taken from CMS5. Irradiated fuel neutron source spectra were developed using ORIGEN-S[11]. Secondary source neutron yields and spectra were determined for neutrons leaving the secondary source assembly using an MCNP photo-neutron model of the secondary source pellets and cladding.

Variance reduction was performed using source biasing, weight windows, and implicit absorption. The fixed source and Keff models used the same geometry and material modeling, only varying the cards needed to run in fixed source or KCODE modes.

Fixed source modeling with MCNP was benchmarked by modeling core on-load sequences and comparing the predicted source range channel response to the measured responses. The comparisons were performed on a relative basis as the MCNP model does not include source range channel detector efficiencies. The MCNP model matched both the change in detector response as a function of source location, source intensity, and subcritical multiplication in the partially-loaded core.

Eigenvalue modeling was benchmarked against measured data from startup physics testing at hot conditions and core design predictions at cold conditions. Eigenvalue cases were converged to within ~80 pcm (1σ). The models showed eigenvalue biases ranging from <100 pcm to 600 pcm, primarily depending on the use of un-irradiated vs. irradiated fuel. It is believed that the increased bias in the eigenvalues calculated for irradiated cores can be attributed to the approximate method of assigning fuel compositions to fuel pins. The biases were compensated for by reporting relative source range detector response as a function of Keff and not soluble boron concentration.

The MCNP models were also used to compute the optional source weighted ex-core detector model radial and axial weights. Fission neutron production rates and intrinsic neutron sources were collapsed into a relative source range response by spatially-weighting, using point kernel response functions and summing the results. The radial and axial point kernel response functions, relative to the ex-core detector located on the south edge and spanning the lower half of the core axially, are shown in Fig. 3 and 4 respectively. It is clear from the figure that ex-core detector signal is primarily driven by edge assemblies in the core.

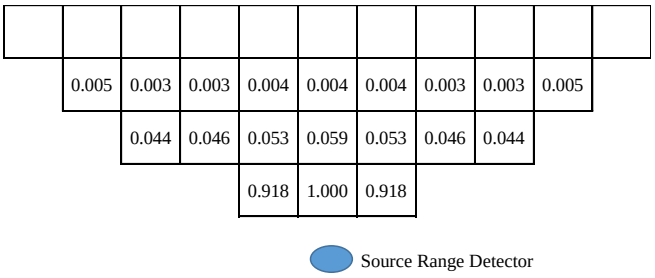


Fig. 3. Assembly-wise ex-core detector radial weight functions for a 3-loop Westinghouse PWR.

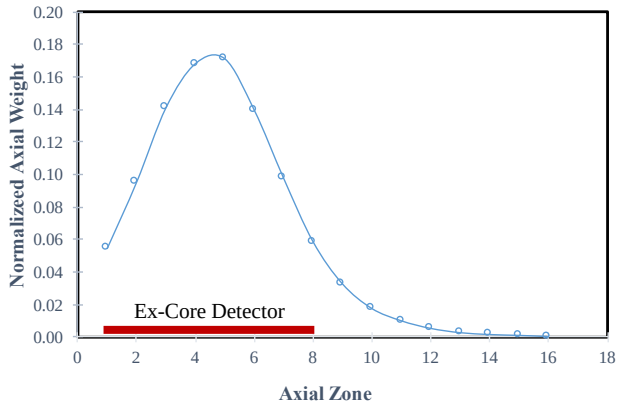


Fig. 4. Ex-core detector axial weight function for a detector located below the core midplane.

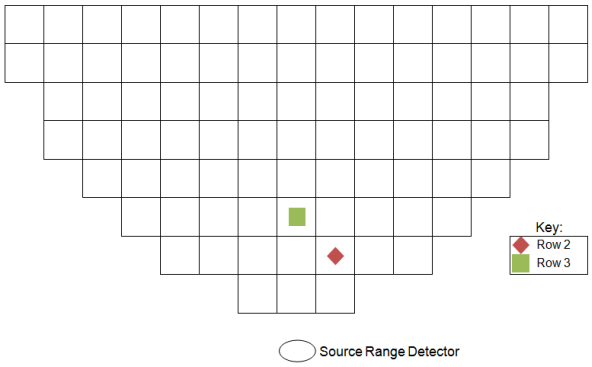


Fig. 5. Secondary Source (SS) and ex-core detector placement.

## III. RESULTS

### 1. MCNP Comparisons

SIMULATE5's combined fixed-source solution and ex-core detector models were verified against the higher-order transport solution from MCNP5.

The MCNP5 benchmark models a hypothetical transient (a boron dilution scenario) in which k-eff increases from far sub-critical ($k_{eff}$=0.91) to just before $k_{eff}$ =1.0. The Inverse Count Rate Ratio (ICRR) for each k-eff is calculated as the ex-core detector response (neutron /cm2·s) for that state point divided into the beginning detector response, similar to constructing a "1/M" plot during reactor startup.

For this particular scenario, a 3D core model, described in Section 2.6, was setup with both MCNP5 and SIMULATE5. The internal neutron sources from once and twice burned fuel in the core were obtained from SIMULATE5 and provided to MCNP5 as an input. The location and the strength of a secondary source, if any in the core, was given from an input. The SIMULATE5 model used four energy groups. This is a low-leakage core, with mostly twice burned fuel assemblies loaded on the core periphery. The Hot Zero Power all-rods-inserted (ARI) state at the beginning of cycle was used to demonstrate the ex-core detector response for three secondary source arrangements as shown in Fig. 5:

1. No secondary source present
2. A secondary source placed two fuel assembly rows away from the ex-core detector
3. A secondary source placed three fuel assembly rows away from the ex-core detector

Fig. 6 shows the 2D, axially integrated fast flux (E > 0.625 eV) distribution for a critical core and for three sub-critical cores with different secondary source arrangements. The fast flux distributions between these cases vary substantially: for a critical core, the flux peaks in the ring two to three assembly pitches away from the edge that have the most reactive assemblies in the core; for a sub-critical core with no external source, the flux is driven by the intrinsic sources of the highly irradiated fuel assemblies; whereas the core containing the external source, the flux peaks at the location of the secondary sources. Note the different scale with each plot; the flux level between these cases differ several orders of magnitude. Other than the critical state, in which the plotted flux was normalized to 1.0e-7% rated power, the sub-critical states show the absolute flux from the solution of the fixed-neutron source equations.

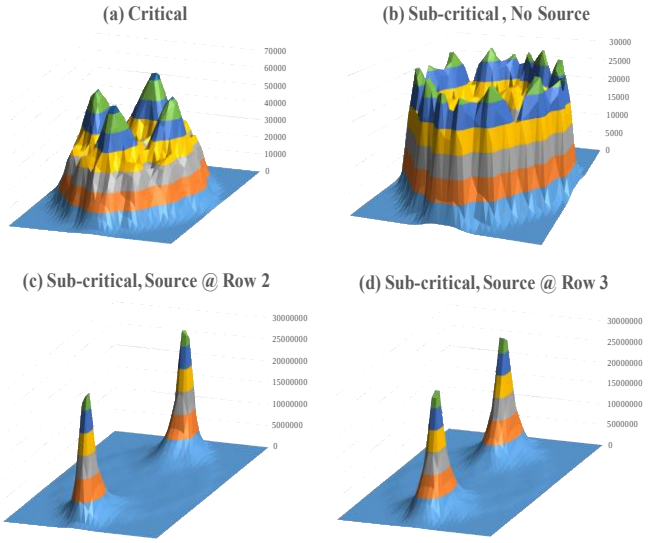


Fig. 6. The 2D fast flux distributions in the core.

In each case, SIMULATE5 ex-core detector responses, computed using the geometrical ex-core detector model, (labeled as CMS5) were compared with results from a corresponding MCNP5 model. The results of these ICRR calculations are presented in Fig. 7. SIMULATE5 does an excellent job of matching the MCNP5 results. Considering numerous modeling approximations with the MCNP5 and SIMULATE5 setups, the small variations in ICRR curve predictions are expected. One example, which is believed to be the primary contributor, is the difference in the intrinsic source distribution in the core: the MCNP model assigns a batch generic intrinsic-neutron sources to all fuel assemblies of a batch, whereas in the SIMULATE5 model, each quarter of an assembly has its own source distributions. This difference can be important for high burnup fuel assemblies loaded on the edges that drive the ex-core detector signal, particularly for the no-source case.

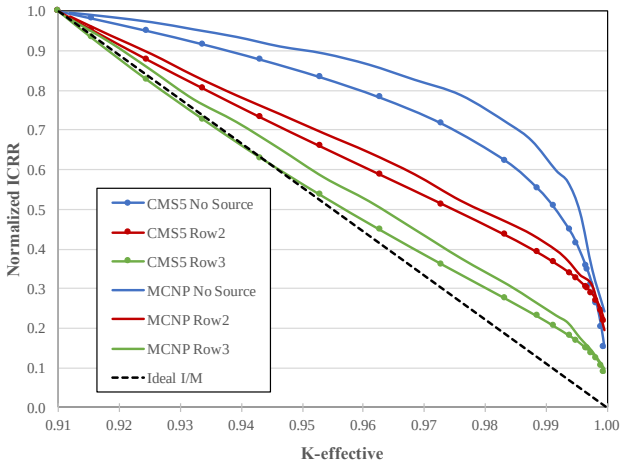


Fig. 7. CMS5 geometric ex-core model versus MCNP5 detector response during a hypothetical boron dilution event.

Note that both the MCNP5 and SIMULATE5 models show a much slower increase in the ex-core detector responses, ICRR, compared to the theoretical "1/M" without a secondary neutron sources in the core. The improvement in the ICRR curve response can be achieved by introducing a secondary source in either row two or three for this particular core design.

The SIMULATE5 calculations were repeated using the source-weighted ex-core detector model, in which the radial and axial source weight functions were taken from the MCNP5 calculations as presented in Fig. 3 and Fig 4. The SIMULATE5 comparisons vs MCNP 5 are presented in Fig. 8. The overall agreement between these models is good. Comparison of two SIMULATE5 ex-core models (Fig. 7 and Fig. 8) revealed that the source-weighted model gives slightly better predictions for cases containing the secondary source and slightly worse prediction for the no-source case relative to the geometrical ex-core detector model. The intrinsic source neutrons have a faster spectrum and higher leakage probability to reach the detector and contribute to the signal than the external source and fission neutrons. The geometrical model, which extrapolates the multi-group flux, directly captures the difference in the intrinsic and external neutron source spectrum, whereas the source-weighted model cannot. It is believed that the change in the ratio of the intrinsic to total source neutrons for each scenario is partially responsible for the detector model predictions. Further study is planned for better understanding of the detector model differences.

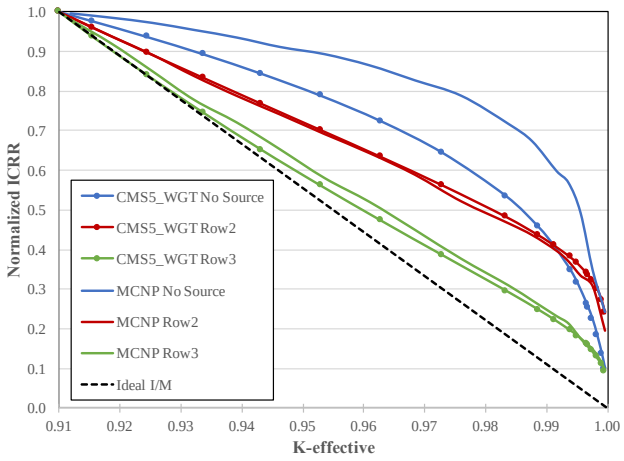


Fig. 8. CMS5 source-weighted ex-core model versus MCNP5 detector response during a hypothetical boron dilution event.

It should be noted that one particular advantage of the geometrical ex-core detector model is that it doesn't require the pre-computed radial and axial source weight functions from a transport calculation, which can be quite time consuming and expensive considering additional time needed with setting up and running such models.

## 2. Plant Measurement Comparisons

The validation of the fixed-source and ex-core detector models of SIMULATE5 was extended for two of the latest cycles of an operating PWR.

Fig. 9 presents the ICRR as computed using measured source range detector (detectors named N31 and N32) responses from the initial approach to criticality for two North Anna cycles. The North Anna Power Station is a dual unit 3-loop Westinghouse NSSS plant. The North Anna Unit 2 Cycle 24 (N2C24) core loading did not have charged secondary sources loaded, while the next cycle, N2C25, did have charged secondary sources in place. The measured detector ICRR state points in the figure occur at the following points where reliable boron concentration chemistry data was available:

1. Shutdown banks withdrawn, after a first dilution (k~0.94)

2. Shutdown banks withdrawn, after a second dilution (k~0.95)

3. Near ARO (D-bank slightly in), immediately before the final dilution to critical (k~0.99)

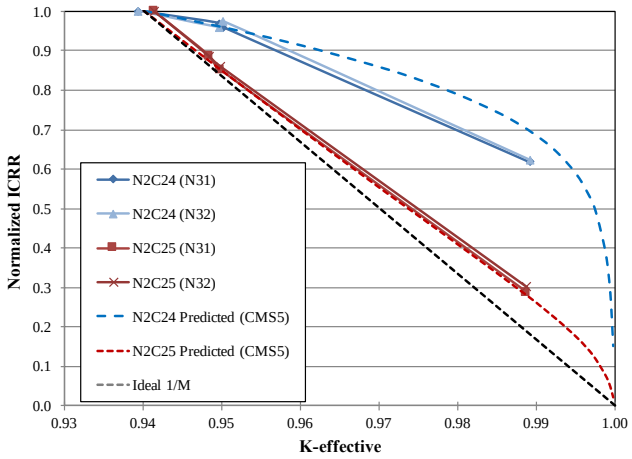


Fig. 9. SIMULATE5 vs measured ex-core detector responses during approach to critical event for N2C24 (Uncharged SS) and N2C25 (Charged SS).

In addition to the measured ICRR data (solid lines), the SIMULATE5 predicted response for both cycles has also been plotted (dashed lines). The SIMULATE5 models employ the geometrical ex-core detector model. Even though the predicted response curves were not constructed with the exact control rod positions used during the bank withdrawal sequence, the predicted response matched well with the measured response for both the N2C24 and N2C25 cores, clearly capturing the improved performance of the detector response when charged secondary sources are used.

## IV. CONCLUSIONS

The fixed-source calculation capability and ex-core detector models implemented in Studsvik's 3D Nodal code SIMULATE5 have been summarized. These models have been validated against the Monte Carlo code MCNP5, for a hypothetical event, and against plant measurements during two approach to critical events of an operating PWR.

It was demonstrated through validation cases that SIMULATE5 accurately predicts the ex-core detector signal during approach to critical events. When one considers the run-time requirements, the cost saving with SIMULATE5 is substantial: a typical SIMULATE5 calculation, of which results are presented in this paper, requires on the order of minutes on a standard quad-core Linux box, whereas the same type of Monte Carlo calculation requires on the order of days. The comparisons of two ex-core detector models, one based on a source weighting model and the other based on extrapolation of the reflector node fluxes to ex-core detector locations with the given detector geometry, showed comparable ICRR curve predictions. The geometrical method simplifies the calculation scheme as it does not require any additional transport code calculations to pre-compute the radial and axial source weight functions.

Both the hypothetical and actual approach to critical events showed that the response of the source range detectors can be significantly improved (i.e., moving the ICRR curve closer to the ideal linear 1/M curve) by introducing the secondary neutron sources back into the core.

These findings demonstrate that SIMULATE5 is an effective tool for the support of operating commercial reactors to predict the ex-core detector signals during various approach to critical events, to find the optimal placement of the secondary neutrons sources in the core and to predict the core sub-criticality.

## REFERENCES

1. W. BOJDUJ, "Source Range Detector Response during Boron Dilution Accident at Shutdown," ANS Annual Meeting, Vol 103, Las Vegas (2010).
2. A. FORD, "Modeling a Source Range Channel Response during a PWR Core On-load Sequence," ANS Annual Meeting, Vol 103, Las Vegas (2010).
3. J. SUN, M-S. YAHYA AND Y. KIM, "A Study on the Optimal Position for the Secondary Neutron Source in Pressurized Water Reactors," *Nuclear Engineering and Technology*, 48 (2016).
4. J. D. RHODES, N. GHEORGHIU, R. M. FERRER, "CASMO5 JENDL 4.0 and ENDF/B- VII.1beta4 Libraries," PHYSOR 2012, Knoxville, Tenn., USA (2012) (CD-ROM).
5. T. BAHADIR, S.-Ö. LINDHAL, S. PALMTAG, "SIMULATE4 Multi-Group Nodal Code with Microscopic Depletion Model," ANS Topical Meeting in Mathematics and Computation (M&C 2005), Avignon, France (2005) (CD-ROM).
6. G.M. GRANDI, "S3K, Models and Methodology," SSP-98/13 Rev7 (2011).
7. H. TOCHIHARA, E. OCHIAI, and T. HASEGAWA, "Reevaluation of Spatial Weighting Factors for Ex-Core Neutron Detectors," *Nucl. Technol*., 58, 310 (1982).
8. "REFUSIM v2.3.5 Methods Description," SSP Technical Note (2007).
9. T. BAHADIR, S.-Ö. LINDHAL, "SIMULATE4 Pin Power Calculations," ANS Topical Meeting in Reactor Physics (PHYSOR 2006), Vancouver, BC, Canada (2006) (CD-ROM).
10. X-5 MONTE CARLO TEAM, "MCNP–A General Monte Carlo N-Particle Transport Code, Version 5-Volume I", LA-UR-03-1987, Los Alamos National Laboratory (2003).
11. SCALE: *A modular Code System for Performing Standardized Computer Analyses for Licensing Evaluations*, ORNL/TM-2005/39, Version 5.1, Vols. I-III (2006).